

## Evidence for Magnetic Interactions between Distant Cations in Yttrium Iron Garnet

P. Novák

*Institute of Physics, Academy of Sciences, Cukrovarnická 10, 162 00 Praha 6, Czech Republic*

J. English, H. Štěpánková, and J. Kohout

*Faculty of Mathematics and Physics, Charles University V, Holešovičkách 2, 180 40 Praha 8, Czech Republic*

H. Lütgemeier and K. Wagner

*Institut für Festkörperforschung, Forschungszentrum Jülich, Postfach 1913, Jülich, D-52425, Germany*

W. Tolksdorf

*Hohenweg 3, Ranstadt, D-63691, Germany*

(Received 7 March 1995)

The NMR spectrum of  $^{57}\text{Fe}$  nuclei in high purity  $\text{Y}_3\text{Fe}_5\text{O}_{12}$  garnet (YIG) is reported. The satellite structure of this spectrum is caused by an antisite defect ( $\text{Y}^{3+}$  ion replacing an  $\text{Fe}^{3+}$  ion). Resolved satellite lines, which correspond to the  $\text{Fe}^{3+}$  ion in six different cation coordination spheres around the defect, are observed. In particular, satellite lines arising from the  $\text{Fe}^{3+}$  ions' distance of which from the defect is as large as 1.07 nm (11th coordination sphere) are identified unambiguously. The results yield information on the range of magnetic interactions in YIG.

PACS numbers: 75.50.Gg, 75.30.Hx, 76.60.-k

It is generally believed that in magnetic insulators the exchange interaction between the magnetic ions decreases rapidly with increasing distance between these ions. Some doubts were cast on the short range of the exchange interaction by the EPR measurements of magnetically coupled pairs in a nonmagnetic matrix. In particular, Henning [1] has shown that there exists a non-negligible superexchange interaction between pairs of  $\text{Cr}^{3+}$  ions in  $\text{ZnGa}_2\text{O}_4$  which are as far as 0.84 nm apart. Until the present work, however, no analogous experiment had been carried out for the magnetic systems themselves. In the present paper we show that in ferrimagnetic garnet  $\text{Y}_3\text{Fe}_5\text{O}_{12}$  (YIG), which is a prototype of the magnetic insulator, there exists a rather large magnetic interaction between the cations which are more than 1 nm apart. The interaction is revealed unambiguously by the change of the hyperfine field acting on the  $^{57}\text{Fe}$  nuclei when its magnetic  $\text{Fe}^{3+}$  neighbor is replaced by a nonmagnetic one ( $\text{Y}^{3+}$  ion on the octahedral sublattice—the so-called Y-antisite defect).

In an ideal YIG,  $\text{Fe}^{3+}$  ions fully occupy tetrahedral ( $d$ ) and octahedral ( $a$ ) positions, while  $\text{Y}^{3+}$  ions enter the dodecahedral ( $c$ ) sublattice. A full description of the crystal structure of garnet is given, e.g., in [2]. The magnetic moments of the  $a$  and  $d$  site  $\text{Fe}^{3+}$  ions are antiparallel, and they lie along the  $\langle 111 \rangle$  direction. For this direction of the magnetic moment all  $d$  sites are magnetically equivalent, while there are two magnetically inequivalent  $a$  sites:  $a_1$  (local  $C_3$  axis parallel to the magnetization) and  $a_2$  ( $C_3$  axis and magnetization lie along different body diagonals). The NMR spectrum of the  $^{57}\text{Fe}$  nuclei then consists of three lines with the ratio of intensities  $d:a_1:a_2 = 6:1:3$ .

If the magnetic  $\text{Fe}^{3+}$  ion is replaced by a nonmagnetic defect, the hyperfine field on Fe nuclei close to the defect is changed. If the change is larger than the NMR linewidth, satellite lines in the NMR spectra appear. The satellite structure is closely related to the symmetry. In order to understand and employ this relation we divide the configurations of defect and resonating nuclei into sets of crystallographically equivalent configurations (CEC). Within each CEC set the configurations are related by the symmetry operations of the space symmetry group  $Ia3d$  of the garnet. When the configuration of the defect and resonating nuclei has no symmetry left, each symmetry operation creates a new configuration. The number of symmetry operations per primitive cell of the  $Ia3d$  group is 48 [3], hence the number of different configurations in corresponding CEC set is also 48. When the configurations still have some symmetry, their number in the CEC set is smaller (no new configurations are created by remaining symmetry operations). For the discussion below, a particularly important CEC set corresponds to a defect and resonating nucleus (both on the  $a$  sites) being on a common  $C_3$  axis. Trigonal symmetry then remains (two rotations  $C_3$  and  $C_3^2$ ) and the number of configurations in this set is  $48/3=16$ .

The configurations within the CEC set differ in their orientation and, eventually, in their position in the primitive cell. If the hyperfine field is isotropic (independent of the direction of magnetization), a single satellite will correspond to each set of CEC. In general, however, the anisotropy of the hyperfine field causes several satellites associated with the same CEC set to appear. To determine the number and relative amplitudes of the satellites we write the general form for the dependence of the reso-

nance frequency  $f_{\text{res}}$  on the directional cosines  $\vartheta_x, \vartheta_y, \vartheta_z$  of the magnetization  $\vec{M}$  (fourth and higher order terms in  $\vartheta_x, \vartheta_y, \vartheta_z$  are neglected):

$$f_{\text{res}} = f_0 + f_{\vartheta}(3\vartheta_z^2 - 1) + f_{\varepsilon}(\vartheta_x^2 - \vartheta_y^2) + f_{xy}\vartheta_x\vartheta_y + f_{xz}\vartheta_x\vartheta_z + f_{yz}\vartheta_y\vartheta_z. \quad (1)$$

For each CEC set we consider a single "trial" configuration, but for all directions of  $\vec{M}$  related by 48 symmetry operations of the garnet symmetry group—the star of directions associated with  $[\vartheta_x, \vartheta_y, \vartheta_z]$ . In the case considered here  $\vec{M}$  is parallel to  $[111]$ , and the corresponding star consists of eight directions parallel to the body diagonals. Using (1) we get four different  $f_{\text{res}}$  for  $\vec{M} \parallel [111]$ :

$$\begin{aligned} f_1 &= f_0 + (f_{xy} + f_{xz} + f_{yz})/3, \\ f_2 &= f_0 + (-f_{xy} - f_{xz} + f_{yz})/3, \\ f_3 &= f_0 + (-f_{xy} + f_{xz} - f_{yz})/3, \\ f_4 &= f_0 + (f_{xy} - f_{xz} - f_{yz})/3. \end{aligned} \quad (2)$$

For a CEC set with configurations having no symmetry left and for  $\vec{M} \parallel [111]$ , 12 configurations contribute to each satellite. We therefore expect that four satellites will appear, each having the same amplitude. For the CEC set whose configurations have the trigonal symmetry we take as the trial configuration the one in which both the defect and the resonating nucleus are on the  $[111]$  axis. The symmetry requires

$$f_{\vartheta} = f_{\varepsilon} = 0, \quad f_{xy} = f_{xz} = f_{yz}. \quad (3)$$

It follows from (1) that this set gives rise to two satellites only. The amplitudes of these satellites are in the ratio 1:3. As there are 16 configurations in this CEC set, 12 configurations contribute to the more intense satellite. Its amplitude is thus equal to the amplitude of the satellites arising from CEC sets with no symmetry, while the less intense satellite has  $\frac{1}{3}$  of this amplitude.

To establish correspondence between a specific satellite line and a particular frequency  $f_i$  in (2) is difficult, as it would require a microscopic model for the hyperfine field. As discussed below, it is much easier to identify the satellites belonging to the same CEC set. Once all these satellites are found we can easily determine the isotropic part  $f_0$  in (3) and also the quantity  $\bar{f}_{\text{trig}}$  which characterizes the magnitude of hyperfine field anisotropy connected with the  $\langle 111 \rangle$  directions:

$$\begin{aligned} f_0 &= (f_1 + f_2 + f_3 + f_4)/4, \\ \bar{f}_{\text{trig}} &= \frac{1}{2\sqrt{3}}(f_{xy}^2 + f_{xz}^2 + f_{yz}^2)^{1/2} \\ &= \frac{\sqrt{3}}{4} \left[ \sum_{i=1}^4 (f_i - f_0)^2 \right]^{1/2}. \end{aligned} \quad (4)$$

We note that for the CEC set with trigonal symmetry  $\bar{f}_{\text{trig}}$  defined in this way is equal to the absolute value of the axial parameter, i.e., to  $|f_{\vartheta}|$  in (1) if the coordinate system with the  $z$  axis  $\parallel [111]$  is chosen.

Rather than discuss the frequency of the satellite lines, we concentrate on the splitting  $d_{\text{sat}}$  between the satellite and the corresponding main line

$$d_{\text{sat}} = f_{\text{sat}} - f_{\text{main}}. \quad (5)$$

The whole discussion above concerning  $f_{\text{res}}$  of the satellites applies also to their splittings  $d_{\text{sat}}$ . In particular, we define the parameters  $d_{\alpha}$  ( $\alpha = \vartheta, \varepsilon, \dots$ ) in analogy with (1) and the parameter  $\bar{d}_{\text{trig}}$  in analogy with (4).

While the satellite pattern—the number and relative intensities of the satellites—is connected with the symmetry of the problem, the magnitudes of splittings between the satellites and the main line are characteristic of a given defect and given CEC set. There are several different microscopic sources of the splitting. The most important mechanisms are believed to be (i) the change of the dipolar field (magnetic ion is replaced by a nonmagnetic one), (ii) the change in the transfer of electrons caused by the substitution, and (iii) the change in the zero point spin deviation. In addition, at nonzero temperature the spin moments which are near to the defect will have different magnitudes compared to the spins which are far from the defect. This is caused by the fact that substitution of a nonmagnetic for a magnetic ion removes several exchange bonds, and, therefore, for spins in the vicinity of the defect the exchange fields are changed.

In our previous paper [4] the results of the NMR study of several nominally pure YIG thin films and polycrystals were described. By comparing the spectra of different samples, several satellite lines caused by an antisite  $\text{Y}^{3+}(a)$  defect were identified. The spectra in [4] exhibit many other satellite lines which are due to yet unidentified defects and/or impurities. The present paper is based on results obtained using a high purity single crystal of YIG grown from the  $\text{BaO}/\text{B}_2\text{O}_3$  flux. The only defects present in this system (in significant concentration) which give rise to the resolved satellites are the above-mentioned Y-antisite defects. The NMR lines are narrower compared to the lines in systems studied earlier [4]. The resolution is therefore better, and more information on Y-antisite defects is obtained.

NMR spectra were measured by the spin-echo method using the phase-coherent spectrometer with an averaging technique and the complex Fourier transformation. The measurements were made at zero external magnetic field. The high rf power was used in order to excite only the signals from the domains. The NMR spectrum measured at temperature 20 K is displayed in Fig. 1. The concentration  $c$  of the antisite defect determined from the ratio of amplitudes of the satellite and corresponding main line [4] is  $c = 0.0074(10)$ . In Fig. 1 the satellites are labeled  $s_{i,j}$ , where  $i$  denotes the CEC set (Table I) and  $j$  is the index differentiating between satellites arising from different configurations in the same CEC set. A comment is needed in order to clear up how the satellites were assigned to the CEC sets. The frequency difference

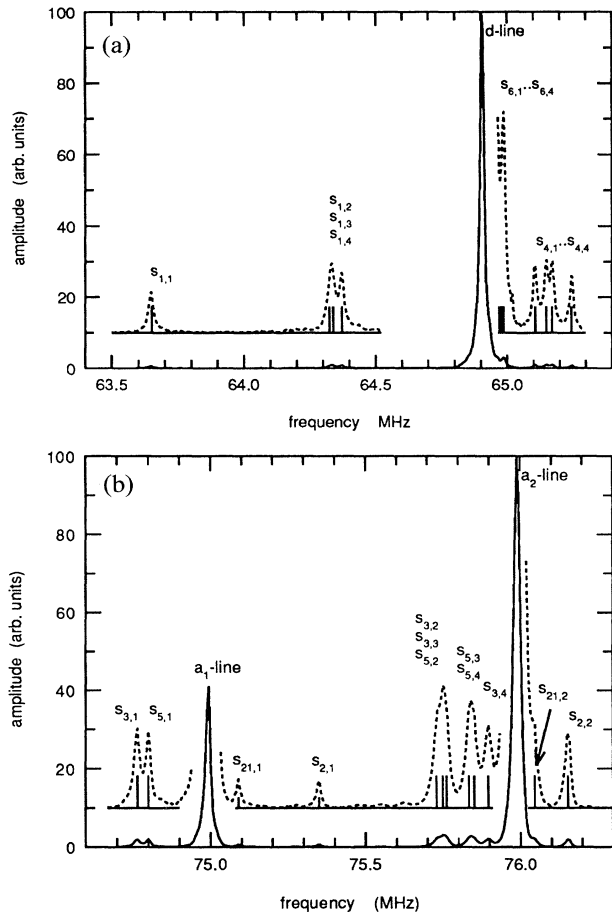


FIG. 1. NMR spectrum of  $^{57}\text{Fe}$  nuclei in YIG at 20 K. For labeling of the satellites, see the text. The dashed curve corresponds to the spectrum magnified  $20\times$  ( $d$  line) and  $10\times$  ( $a$  lines). Vertical bars denote positions of the satellites.

between the  $d$  and  $a_i$  ( $i = 1, 2$ ) lines is much bigger than the splittings between the satellite and corresponding main line. It is therefore easy to distinguish satellites belonging to the  $d$  line from those of  $a_1$  and  $a_2$  lines.

Next comes the more subtle problem of differentiating between the CEC sets which correspond to  $\text{Fe}^{3+}$  ions located on the same sublattice. We used two ways when establishing this correspondence. To some extent we can rely on the fact that, whatever the mechanism causing the change of the hyperfine field, the change should decrease with increasing distance between the defect and the resonating nuclei. Caution is needed, however, when applying this rule, as it is often the angles between the bonds, rather than the distance, that decide which interaction is stronger. An example relevant to our problem is provided by  $\text{Ca}_3\text{Fe}_2\text{Ge}_3\text{O}_{12}$  garnet—as shown in [5] the superexchange interactions between nearest and second nearest  $\text{Fe}^{3+}(a)$  neighbors (corresponding to CEC sets 3 and 5 in Table I) are comparable in this system.

TABLE I. Satellites in the NMR spectrum of YIG containing the Y-antisite defects.  $N_{\text{CEC}}$  is the index of the CEC set,  $N_{\text{c.s.}}$  is the corresponding cation coordination sphere of the defect, Subl. means the sublattice of resonating Fe nuclei, and  $R$  (nm) is the distance between the resonating nuclei and the defect. Values of  $d_0$  and  $\bar{d}_{\text{trig}}$  (in MHz) were deduced from experiment at  $T = 4.2$  K. Also given is the calculated dipolar contribution  $d_{\text{trig}}^{\text{dip}}$  to  $\bar{d}_{\text{trig}}$ . Bold lines correspond to sets of CEC having the trigonal symmetry. An asterisk means that the correspondence between experimentally observed satellites and the CEC set is only tentative (see text).

$N_{\text{CEC}}$	$N_{\text{c.s.}}$	Subl.	$R$	$d_0$	$\bar{d}_{\text{trig}}$	$d_{\text{trig}}^{\text{dip}}$
1	1	$d$	0.346	-0.730	0.265	0.107
<b>2</b>	<b>2</b>	$a$	<b>0.536</b>	<b>0.213</b>	<b>0.072</b>	<b>0.041</b>
3	2	$a$	0.536	-0.205	0.057	0.041
4*	3	$d$	0.556	0.264	0.044	0.029
5	4	$a$	0.619	-0.179	0.030	0
(6,7)*	5	$d$	0.709	0.079	0.006	0.013
8-10	6	$d$	0.833			
11-12	7	$a$	0.875			
13	8	$d$	0.941			
14-17	9	$a$	1.026			
18-20	10	$d$	1.038			
<b>21</b>	<b>11</b>	$a$	<b>1.072</b>	<b>0.061</b>	<b>0.017</b>	<b>0.005</b>

When assigning the satellites to a particular CEC set, the temperature dependence of NMR spectra is very helpful. We expect the temperature dependence of splittings between satellites and the main line of all crystallographically equivalent configurations to be similar as it is mainly governed by the change in magnitude of the  $\text{Fe}^{3+}$  electronic magnetic moment. The magnitudes of magnetic moments of  $\text{Fe}^{3+}$  ions on crystallographically equivalent positions can only differ because of the anisotropy of the exchange interaction—this, however, is believed to be negligible in the system considered.

Identification of  $s_{1,k}$  ( $k = 1, \dots, 4$ ) satellites is relatively straightforward. Corresponding splittings (Table I) are significantly larger compared to other  $d$  line satellites, and their resonance frequencies decrease faster with increasing temperature than  $f_{\text{res}}$  of the main line and  $f_{\text{res}}$  of satellites from other CEC sets. This may be easily understood, as the spins of corresponding  $\text{Fe}^{3+}(d)$  ions are subjected to a smaller exchange field [one of the four exchange bonds to nearest  $\text{Fe}^{3+}(a)$  ions is missing due to  $\text{Y}^{3+} \rightarrow \text{Fe}^{3+}(a)$  substitution]. On the other hand, the assignment of experimentally observed satellites to the fourth and sixth CEC sets relies on the above mentioned dependence of the interaction on the distance and it must therefore be taken as tentative only.

The temperature dependence of the splittings corresponding to  $a_1$  and  $a_2$  line satellites is displayed in Fig. 2. The different temperature dependence of the splittings of satellites belonging to different CEC sets may be clearly seen from this figure. The character of the dependence is

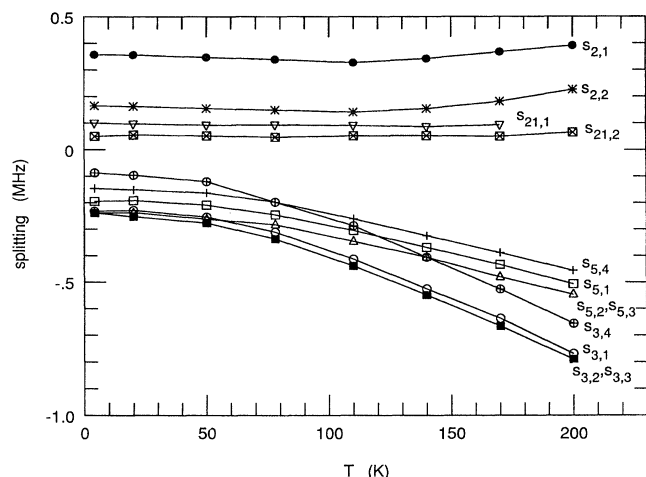


FIG. 2.  $a_1$  and  $a_2$  lines. Temperature dependence of the splittings between satellites and corresponding main line. Full curves serve as a guide for the eyes only.

interesting. The magnetic moments of  $\text{Fe}^{3+}(a)$  ions are parallel and  $\text{Fe}^{3+}(a)\text{-Fe}^{3+}(a)$  exchange interactions are known to be antiferromagnetic [5]. We would therefore expect an increase of the exchange field due to the missing unfavorable interaction, and, consequently, slower decrease of satellites  $f_{\text{res}}$  compared to the main lines. It may be seen from Fig. 2 that for the third and fifth CEC sets these expectations are in conflict with the experiment. We can—at least qualitatively—understand this behavior as being caused by the interaction with  $\text{Fe}^{3+}(d)$  ions which are affected by the defect. The moments of these  $\text{Fe}^{3+}(d)$  ions decrease faster with increasing temperature, and this causes a decrease in the exchange field felt by their  $\text{Fe}^{3+}(a)$  neighbors. Inspection of the garnet crystal structure shows that  $\text{Fe}^{3+}(a)$  ions from the second, fifth, and third CEC set have zero, one, and two affected  $\text{Fe}^{3+}(d)$  neighbors, respectively. This explains the different temperature behavior of  $f_{\text{res}}$  corresponding to these sets and it leads us to the assignment of satellites to the third and fifth set.

Our most important result is the identification of satellites  $s_{2,1}$  and especially  $s_{21,1}$ , which is straightforward and unambiguous. As seen from Fig. 1 the amplitude of these satellites equals  $\frac{1}{3}$  of the amplitude of other satellites present in the spectrum. In accord with the above discussion  $s_{2,1}$  and  $s_{21,1}$  must therefore correspond to defect and resonating nuclei being on the common trigonal axis, which is parallel to the magnetization. To

be sure that  $s_{21,1}$  cannot be caused by some unidentified defect which would incidentally give a satellite with this amplitude, we examined the spectra obtained earlier on other nominally pure YIG systems [4]. In all cases—within the experimental uncertainty—the satellite  $s_{21,1}$  is detected with the correct amplitude. We also note that  $s_{2,1}$  and  $s_{21,1}$  cannot be interchanged, as the configuration which gives rise to  $s_{21,1}$  corresponds to the twice-repeated configuration of  $s_{2,1}$ . Hence the splitting for  $s_{2,1}$  must be larger than the splitting for  $s_{21,1}$ , which makes the identification unambiguous. We conclude therefore that the interaction which causes the change of the hyperfine field has a surprisingly long range.

Though the detailed mechanism of this interaction is not clear there is a strong indication that it arises from electron transfer, i.e., it is connected with a superexchange interaction. First, we note that the splitting is strongly anisotropic. It is difficult to believe that zero point spin deviation could cause an anisotropic splitting as the exchange in YIG is to a good approximation isotropic. Moreover, as seen from Table I, the calculated dipolar contribution  $\bar{d}_{\text{trig}}^{\text{dip}}$  to the anisotropy is substantially smaller than  $\bar{d}_{\text{trig}}$  deduced from the experiment. Therefore, electron transfer must be an important and probably dominant mechanism.

The results obtained present a challenge to the theory of the hyperfine field and electronic structure of magnetic oxides. It would be interesting to see whether the exchange bond model [1,6] could provide a qualitative explanation of the strong, long range interaction of cations on the common trigonal axis. The data collected represent a rich set of information on the behavior of a Heisenberg system containing a nonmagnetic defect. It can therefore be used to test corresponding theoretical models.

This work was supported by the grant of the Czech Grant Agency No. 202-93-0382 and by German-Czech scientific cooperation Grant No. WTZ x242.24.

- [1] J. C. M. Henning, Phys. Rev. B **21**, 4983 (1980).
- [2] G. Winkler, *Magnetic Garnets* (Vieweg and Sohn, Braunschweig, 1981).
- [3] *International Tables for X-Ray Crystallography* (Kynoch, Birmingham, 1952).
- [4] K. Wagner *et al.*, J. Magn. Magn. Mater. (to be published).
- [5] T. Brueckel *et al.*, Z. Phys. B **72**, 477 (1988).
- [6] K. Dwight and N. Menyuk, Phys. Rev. **163**, 435 (1967).